MINI-RF GLOBAL AND POLAR S-BAND MAPS OF THE VARIATION IN THE MOON'S REGOLITH DIELECTRIC CONSTANT. S. Shukla[1,2], A. Maiti[2], G. W. Patterson[3], P. Prem[3], J. T. S. Cahill[3], B. J. Thomson[4], V. A. Tolpekin[5], and S. Kumar[1], [1]Indian Institute of Remote Sensing, ISRO, Dehradun, Uttarakhand, India, [2]Faculty ITC, University of Twente, Enschede, The Netherlands, [3]Johns Hopkins University Applied Physics Laboratory, Laurel, MD, [4]University of Tennessee, Knoxville, TN, and [5]ICEYE, Espoo, Finland.

Introduction: The objective to 'return to the Moon' has stimulated a paradigm shift in our understanding of physical properties of the lunar surface. With the current state-of-the-art radar technology, it is possible to characterize distinct geologic features contained within near surface and subsurface regolith environments that could be of interest for both science and necessary for human or robotic exploration. A fundamental factor in evaluating the radar response from such features and the mediums that make them is dielectric constant. This physical property gives crucial information about the distribution of materials within the regolith useful for unraveling the origin and evolution of the lunar features. Moreover, dielectric content aids in the precise identification of volatiles trapped within different stratigraphic layers at multiple depths. From a radar science perspective, Earth-based analyses provide significant understanding about lunar geologic history (for instance, [1-3]), however the datasets used are limited to the lunar nearside. A more global perspective can build upon our existing knowledge and facilitate new scientific perspectives of lunar processes that may be cornerstones for a better understanding of inner solar system evolution. In this regard, the Miniature Radio Frequency (Mini-RF) instrument on board Lunar Reconnaissance Orbiter (LRO) presents valuable insights into the physical nature of the lunar regolith, volatile characterization, and landing site hazard assessment at global scale [4, 5]. Here, we showcase spatially semi-controlled Mini-RF global and controlled Mini-RF polar S-band maps of the dielectric constant.

Instrument: Mini-RF instrument is a side-looking, hybrid-polarized, synthetic aperture radar (SAR) operating in circular transmit, linear receive mode at 12.6 cm (S-band) or 4.2 cm (X-band) wavelengths with an incidence angle of ~47° [5-7]. The spatial resolution is 150 m (baseline) and 30 m (zoom). Mini-RF has the capability to determine all four Stokes parameters, which are a quantitative representation of polarized radar energy scattered from the lunar surface [6-9]. Traditionally, the dual polarized imaging systems only tend to produce one or the other of the two real Stokes parameters [9]. However, Mini-RF collects all four parameters for us to subsequently generate comparative and complementary data products to the Earth-based analyses. In this study, our focus is primarily on deriving the horizontal and vertical components of the electric field from S-band Stokes parameters.

Method: We have developed a two layer lunar regolith model that incorporates five basic mechanisms: (a) surface scattering from top regolith; (b) volume scattering from buried inclusions; (c) subsurface scattering from bedrock; (d) subsurface-volume scattering; and (e) volume-subsurface scattering [10]. The radar backscatter is computed by parameterizing Integral Equation Model as a function of frequency, roughness, dielectric constant, $FeO+TiO_2$ content, regolith thickness, incidence angle, and buried rock abundance [11]. Rayleigh parameters are extracted for estimating absorption, scattering, and transmission losses of the radar signal when interacting with the regolith at different depths [12]. The developed forward model does not consider multiple scattering between the buried inclusions or the coherent backscatter opposition effect. In order to understand the complex and non-linear relation of radar backscatter with physical parameters, we have developed a novel deep learning based inversion model to retrieve the dielectric constant in a robust and reliable manner benchmarked against the lunar sample drive core measurements [10]. The inputs are horizontal and vertical polarized radar albedo, incidence angle, and frequency, whereas the outputs comprise the real and imaginary part of dielectric constant. For testing, we have used the Mini-RF S-band global and polar data products.

Results and Discussion: The Mini-RF derived maps suggest a wide range of dielectric constant values for both real and imaginary parts, which are in strong agreement with the laboratory-based analyses of the Apollo samples. A major advantage of these maps is to effectively understand and differentiate the physical character of the regolith across different lunar terrains at meter to decimeter vertical scales [13].

Semi-controlled Global Mapping: In Figure 1a-b, we observe significant dielectric contrast between nearside Procellarum KREEP Terrane (PKT) and farside Feldspathic Highland Terrane (FHT). This can be attributed to a relatively smoother texture of PKT mare basalt flows with high TiO_2 content, thereby resulting in radar attenuation and thus low dielectric constant. However, when the roughness measurable at radar wavelength increases, in case of FHTs, the radar returns from subsurface tends to decrease with a surge in dielectric constant values. Moreover, it currently appears not practically possible to discriminate the exact boundaries of the South Pole Aiken (SPA) basin from

the FHT on dielectric grounds, even though the former is compositionally distinct from the latter [13, 14]. We notice a dielectric elevated sub-region within the SPA basin, possibly due to the high density of cm- to m-scale scatterers and unweathered ejecta deposits that limits radar penetration. We further observe peculiar hotspots with high dielectric values around low dielectric regions. This suggests the possible contribution of buried rocks of ~2 cm covered by thin low dielectric regolith media not clearly distinguishable in the S_1 image. Such information demonstrates the potential of our inversion model to capture minute backscatter differences due to buried volumes and subsurface.

Controlled Polar Mapping: In Figure 1c-d, we observe a higher dielectric contrast in the south pole on average relatively to the north pole. In particular, the permanently shadowed regions (PSRs) near south polar craters of Cabeus, Faustini and Shackleton display intriguing and complex dielectric characteristics with large spatial variations compared to other terrains. Such physical character of the PSRs warrants further investigation augmented with other Mini-RF derived products for reliable inference. Also, we notice a significant surge in dielectric contrast around the ejecta of the north polar crater Anaxagoras, easily distinguishable in the map. The behavior may be due to the wavelength scale heterogeneities present in the freshly excavated rocks by the large crater Goldschmidt in the east. The polar regions further exhibit a lower imaginary part of the dielectric constant compared to the equatorial regions, suggesting higher proportion of rocks in the mid-latitude regoliths with the possible increment in fractional volume of ice particles as we go near the poles. The analysis offers an excellent opportunity to strengthen our understanding about lunar volatiles that are expected to exhibit distinct radar response based on the variations in dielectric properties.

References: [1] Ghent R.R. et al. (2005) *JGR, 110,* E02005. [2] Thompson T.W. et al. (1974) *The Moon, 10,* 87-117. [3] Campbell B.A. et al. (2007) *IEEE TGRS, 45,* 4032–4042. [4] Nozette S. et al. (2010) *Space Science Reviews, 150,* 285. [5] Cahill J.T.S. et al. (2014) *Icarus, 243*,173–190. [6] Carter L.M. et al. (2009) *JGR, 114*, E11004. [7] Campbell B.A. et al. (2009) *JGR, 114,* E01001. [8] Raney R.K. (2006) *IEEE, 3,* 317- 319. [9] Campbell B.A. et al. (2009) *GRL, 36,* L22201. [10] Shukla S. et al. *Earth and Space Sci.*, in press. [11] Fa W. et al. (2011) *JGR, 116,* E03005. [12] Fung A.K. (1994) *Artech House, Boston*. [13] Spudis P.D. et al. (2010) *GRL, 37,* L06204. [14] Cahill J.T.S. et al. (2011) *LPSC XLII*.

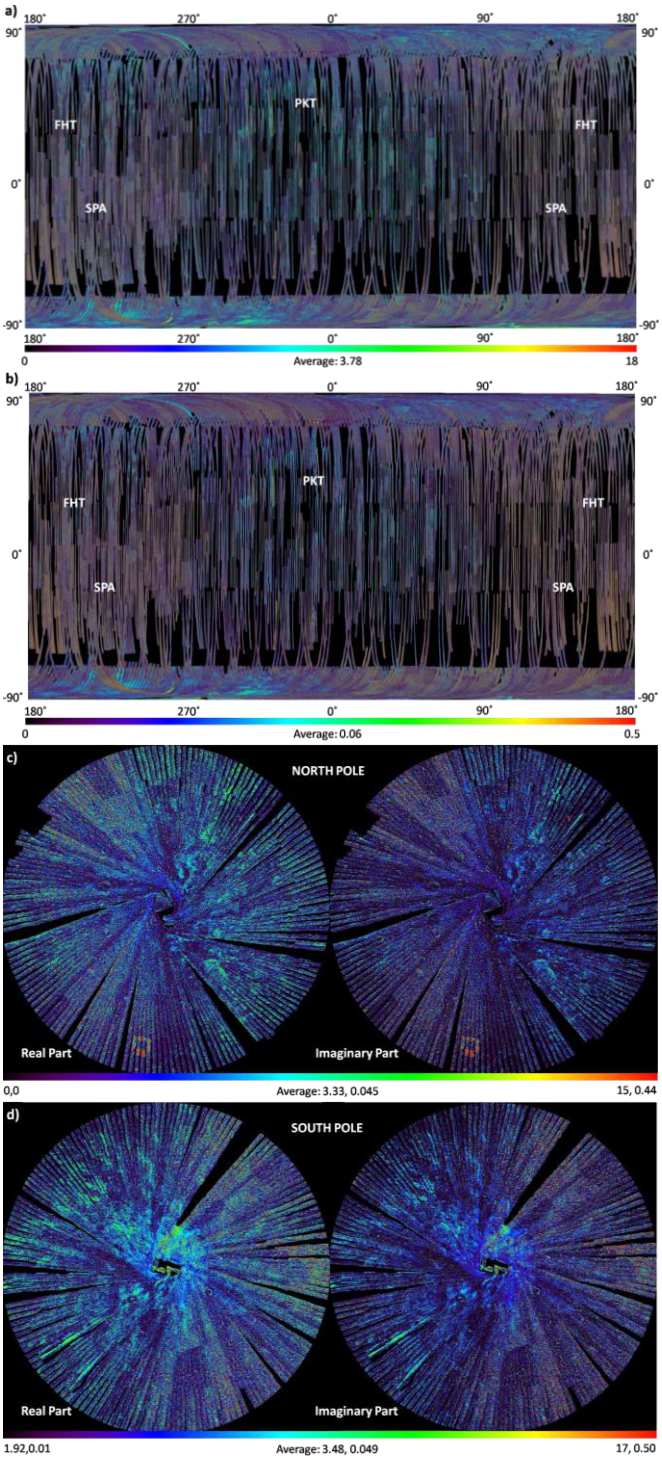

Figure 1. Mini-RF global S-band map of a) real part and b) imaginary part of the dielectric constant (128 pixel/degree). Mini-RF polar S-band maps of the c) North pole, d) South pole (512 pixel/degree). Note: Latitudinal extent of the polar maps is 70˚ to 90˚ at each pole.